ISTS 2006-d-35

TRMM ON-ORBIT PERFORMANCE REASSESSED AFTER CONTROL CHANGE

Stephen Bilanow[(1)] and Steven Slojkowski[(2)]
25th International Symposium on Space Technology and Science, and
19th International Symposium on Space Flight Dynamics
[(1)] SAIC, c/o NASA GSFC Code 610.2 Greenbelt MD 20771, USA
(E-mail: Steve.Bilanow@gsfc.nasa.gov)
[(2)] a.i. solutions, Inc., c/o NASA GSFC Code 595. Greenbelt MD 20771, USA

Abstract

The Tropical Rainfall Measuring Mission (TRMM) spacecraft, a joint mission between the United States and Japan, was launched from the Tanegashima Space Center, Japan on November 28, 1997, and transitioned in August, 2001, from an operating altitude of 350 kilometers to 402.5 kilometers. Due to problems using the Earth sensor at the higher altitude, TRMM switched to a backup attitude control mode. Initially TRMM controlled pitch and roll to the local vertical using Earth horizon measurements while using yaw gyro data to propagate yaw between updates using Sun sensors. After the orbit boost, a 6-state Kalman filter used 3-axis gyro data with Sun sensor and magnetometer data to estimate onboard attitude and gyro rate biases. To better evaluate the onboard pointing performance, roll attitude errors were independently estimated using science instrument radar data, providing a novel insight into various correlations and patterns in the attitude errors. Originally the backup Kalman filter control mode was intended to meet a degraded attitude accuracy of 0.7 degrees; however after improving the onboard ephemeris accuracy and adjusting an onboard magnetometer calibration, it proved possible to meet the original 0.2 degree accuracy requirement.

1. Introduction

The TRMM project was conceived to improve global analysis of rainfall, especially in the tropics over oceanic areas where few measurements had been available. TRMM data has exceeded expectations in providing improved estimates of tropical rainfall amounts which are key to global circulation models, and has also provided many new scientific results [1]. The mission lifetime has been extended, assuring continued scientific benefits, as well as improved operational forecasting benefits for many years.

TRMM flight operations are supported at the National Aeronautics and Space Administration (NASA) Goddard Space Flight Center (GSFC). Analysis of the TRMM attitude performance has been supported by the Flight Dynamics Analysis Branch, and by the Global Change Data Center with responsibility for assuring the science data geolocation accuracy. Results from science instrument data has provided useful feedback on the attitude performance, as presented here.

1.1 Precipitation Radar (PR)

A key instrument on TRMM, the Precipitation Radar (PR), was provided by the Japan Aerospace Exploration Agency (JAXA). It is the first space-based radar for measuring the vertical structure of rainfall. Fig. 1 shows PR measurement of a "hot tower" associated with hurricane intensification [2].

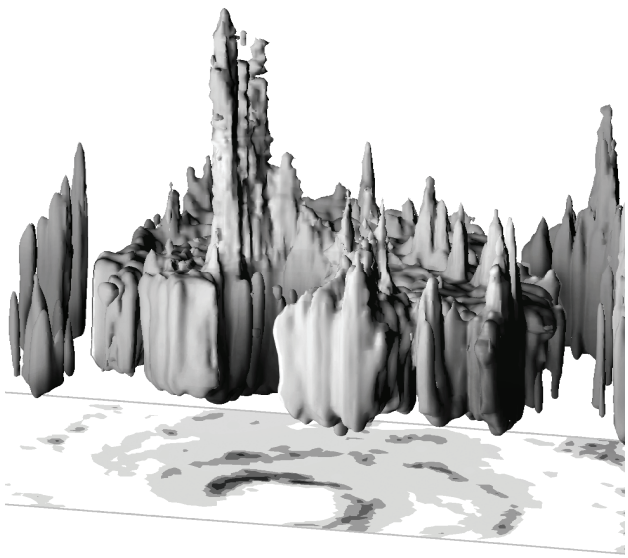

Fig. 1. 3D rainfall structure of Hurricane Bonnie (1998) observed by the TRMM Precipitation Radar

Since the radar detects the surface echo as well as rain, its measurements were used to provide an independent estimate of the roll of the spacecraft by sensing the difference in the surface distance on the left and right sides of the spacecraft flight direction.

1.2 Mission lifetime and orbit boost

TRMM was originally designed for a 3 to 5 year lifetime but, after a change in operating altitude in August 2001, the mission could continue through 2012. TRMM flies in a relatively low orbit to enable the radar measurement of rainfall, so the mission lifetime is limited by the available hydrazine propellant to maintain a roughly constant orbit altitude (within about +/- 1 km in mean semi-major axis). Atmospheric drag on the spacecraft is higher at lower altitudes, and also increases during periods of high solar activity, which heat and expand the upper atmosphere.

In 2001 various options were studied for extending the mission lifetime, and the decision was made to boost the operating altitude from 350 to 402.5 kilometers (km). The choice of 402.5 km was determined by the next higher altitude at which the PR would work, given the designed pulse repetition rate. Key orbit parameters and changes after the boost are summarized in Table 1.

Table 1. Key Orbit Parameters and Changes

Orbit Parameter	**Pre-boost** *(Dec 8, 1997 to Aug. 7 2001)*	**Post-boost** *(Aug 20, 2001, to present)*
Inclination	35 degrees	
Target Altitude (Semimajor axis minus equatorial Earth radius)	350 ± 1.25 km	402.5 ± 1 km
Orbit Period	91.3 minutes	92.4 minutes
Precession Rate	-6.78 deg./day	-6.60 deg./day

Figure 2 displays the TRMM lifetime predictions based on July 2005 solar flux predictions. If the next solar activity maximum is sooner and +2 sigma higher than predicted, then TRMM will re-enter sooner as shown. The actual fuel remaining is estimated from telemetry using a Pressure-Volume-Temperature (PVT) method. Also shown is the TRMM lifetime which would have resulted had TRMM not been boosted to a 402.5 km orbit in August 2001. If TRMM had remained at 350 km it would have depleted its hydrazine by June 2003. A plan was developed to potentially perform a controlled reentry into the Pacific Ocean using 138 kg of fuel. However, the decision was made to use this fuel for an extended mission lifetime. In discussions, the global benefits from improved forecasting of severe weather were counterweighed against the added global risk from debris possibly surviving reentry.

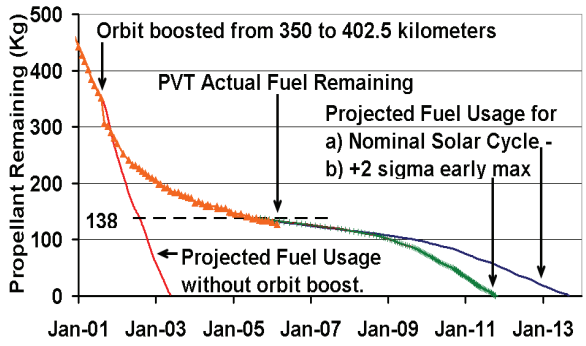

Fig. 2. TRMM orbit lifetime estimates

1.3 Attitude Control System (ACS) changes

TRMM attitude sensors are summarized in Table 2, along with a brief description of how they were used in normal control before and after the orbit boost.

Table 2. ACS Sensors Before and After Orbit Boost as used during routine science data collection

Attitude Sensors	**Pre-boost**	**Post-boost**
ESA, (Earth Sensor Assembly) static 4-quadrant sensor	Used for pitch and roll	(not used)
DSS, (Digital Sun Sensor) two 2-axis sensors	Used for yaw (yaw updated each orbit using each DSS and propagated with yaw gyro)	Used in Kalman filter (solving for attitude and gyro biases with long time constant, with DSS weighted over TAM)
IRU (Inertial, Reference Unit) rate integrating gyros, redundant on each axis		
TAM (Three Axis Magnetometer)	(not used)	

It proved valuable for TRMM to have a backup control mode which did not use the ESA. This contingency mode was added late in the TRMM development cycle after concerns were raised about possible ESA sensitivity to degradation from atomic oxygen causing fogging of its lenses [3]. The onboard flight software was adapted from another mission with some simplifications and modifications to reduce the computational burden on the onboard processor and to use different attitude sensors [4].

A diagram of the TRMM spacecraft in Fig. 3 shows the nominal coordinate system. It also shows the location of the science instruments, the ESA, the solar panels, and the High Gain Antenna.

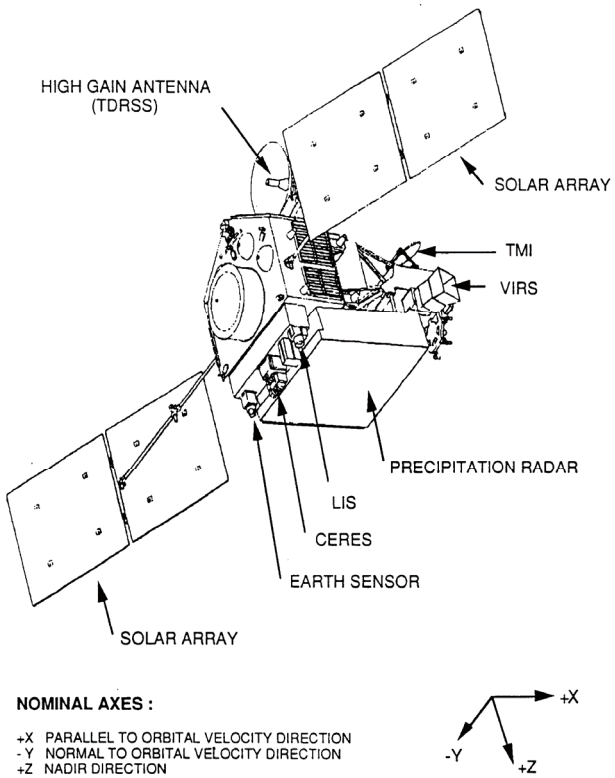

Fig. 3. TRMM spacecraft

1.4 PR roll measurements

Fig. 4 shows the geometry for roll measurement using the PR science instrument [5]. The radar range bin for the maximum surface echo is computed in the PR standard algorithms, and gives an estimate of the distance, D, to the surface. Roll, ϕ, is essentially proportional to the difference, Δ, in the distance to the surface on the two sides of the instrument swath. PR has 49 beam paths scanning about +/- 17 degrees of the nadir direction, with 0.7 degrees between beam directions.

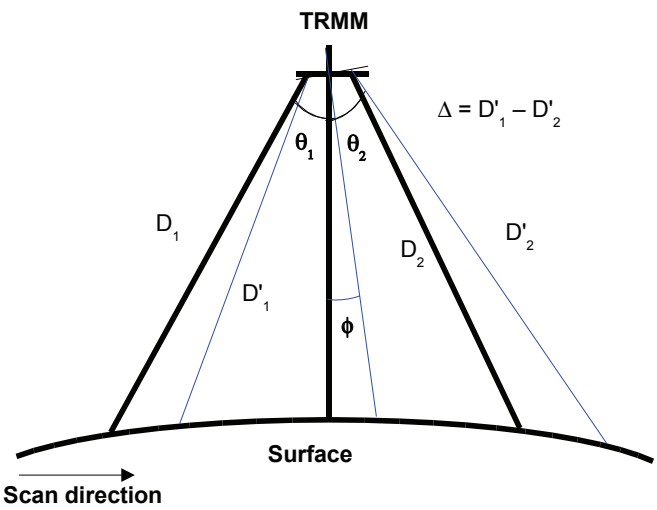

Fig. 4. Geometry for PR roll estimate (not to scale)

In practice, averages of six rays at each edge of the scan were taken to reduce the noise. The sensitivity of the difference to roll was calculated as 3.65 km/deg at 350 km, and 4.2 km/deg at 402.5 km altitude. The small variation in that sensitivity as the geodetic altitude of the spacecraft changed (by about +/- 5 km) around each orbit was ignored since it has less than 2% effect on the roll. Also, nonlinearity in the relationship is unimportant here as the roll variation is generally less than a few tenths of a degree. These measurements were generally used only over ocean areas to avoid effects from surface topography. Although noisy for short-term observation, the PR data illuminated various aspects of the TRMM pointing performance and proved key to evaluating the roll errors in the period after the orbit boost.

1.5 Sun elevation (β) variation, and yaw turns

With a 35 degree inclination orbit, which precesses at about -6.7 degrees per day, there is a 46-day cycle in the Sun's elevation in the orbit plane and in the Sun's phase relative to the orbit ascending node. The elevation is also called the beta (β) angle. β also varies on an annual cycle due to the Earth's 23.5 degree tilt relative the ecliptic plane of the Earth's orbit around the Sun, so that the peak β angles for TRMM are +/- 58.5 degrees. A sample of the β variation over two years is shown in Fig. 5. The variation in the Sun geometry also affects some systematic errors in the attitude estimation, so it is useful to understand these periodic patterns.

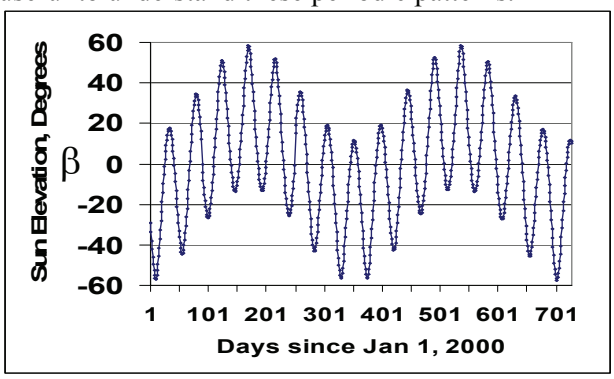

Fig. 5. Solar β angle variation over two years

An important aspect of attitude control support for TRMM are the yaw turns required every 2 to 4 weeks, in order to keep the +Y side of the spacecraft in shadow for thermal control. The 180 degree yaw turns are planned each time β passes through zero. On an orbital basis the Sun basically traces a cone of half-angle β about the body -Y axis, which aligns nearly parallel or anti-parallel to orbit normal.

2. Pre-boost ACS Performance

The performance of the initial, pre-boost control was reported previously [6], however it is reviewed here with respect to roll pointing accuracy with information provided by the PR data, and a few previously unreported aspects are noted.

2.1 Orbits with ESA Sun or Moon interference

Prior to the orbit boost, the largest attitude errors with normal mission operations were typically due to occasional Sun or Moon interference in the ESA. During predicted interference periods, the ACS switched from 4 to 3-quadrant ESA use, and often the 3-quadrant control was less accurate. On rare occasions the ACS changed to 2-quadrant use due to interference from both the Sun and Moon.

A sample 1-orbit span with Sun interference is shown in Fig. 6 illustrating the onboard reported roll, a PR data derived roll, and a ground computed gyro-propagated roll. This was one of the larger disturbances from Sun interference effects.

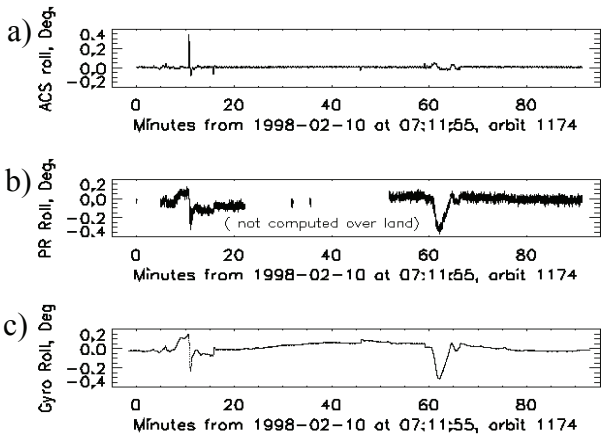

Fig. 6. Pre-boost orbit with Sun interference

Since the momentum wheels control the attitude to the onboard estimate, the onboard reported attitude (Fig. 6a) is practically always close to zero. Sudden jumps in the estimated roll show up as spikes in the reported attitude, and the control quickly responds, within tens of seconds, to null the pointing (details are illustrated in Fig. 8). The PR estimated roll (Fig. 6b) tracks well with an estimate of the roll history propagated using gyro data (Fig 6c), demonstrating the basic reliability of the PR roll observations.

2.2 Frequency and amplitudes of ESA errors

The Sun interference in the ESA quadrants occurs when β (see Fig. 3) is in the range of 35 to 55 degrees. This occurred every orbit for several days at a time, a few times each month. To get a global picture of the frequency and magnitude of these excursions, and also to quality assure that no other unknown attitude excursions were occurring, gyro data was processed from each orbit to roughly track the relative short term motions. The accumulated angles from each axis of the rate-integrating gyro output was subtracted from a linear fit and then fit with a second order orbit period Fourier series to take out the expected drift and periodic motions from geodetic Earth pointing control. The maximum and minimum of the residuals for the roll axis for one year are shown plotted in Fig. 7. The effects of ESA interference show up as an extended range above the usual min-max residual range per orbit. The regular pattern of the errors is consistent with β variation patterns. Errors are sometimes larger than 0.2 deg. in pitch or roll, but usually less. Because the quadrants view along diagonals to the body X and Y axes, coupled pitch and roll offsets occur with 3 quadrant control.

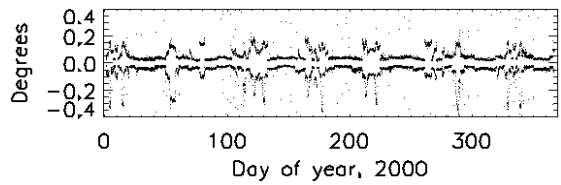

Fig. 7. Range of motion from ESA interference

2.3 ESA mode transition toggling

Small jumps in the onboard attitude were encountered when switching from ESA 4 to 3-quadrant control. These switches were based on an onboard calculation of the predicted region of interference. Since this calculation used the instantaneous onboard attitude estimate as input, and since the switch in quadrant usage affected the onboard attitude in the next control cycle, this sometimes resulted in a toggling back and forth in the onboard attitude at the transition. This is illustrated in Fig. 8, which zooms in on the first spike seen in Fig. 6a. Although not a significant problem, it is noted that the mode transitions could have been filtered from effects like this.

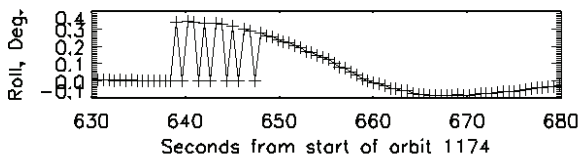

Fig. 8. Toggling between ESA 4 or 3 quadrant use

2.4 Early mission average roll bias shifts

The average PR-measured roll bias from each orbit is shown in Fig. 9 for the first 6 months of the mission. All of the shifts in the average bias that are seen above the noise level are associated with yaw turns of the spacecraft (done when the β angle passes though zero), except for the very first one which is associated with calibration changes.

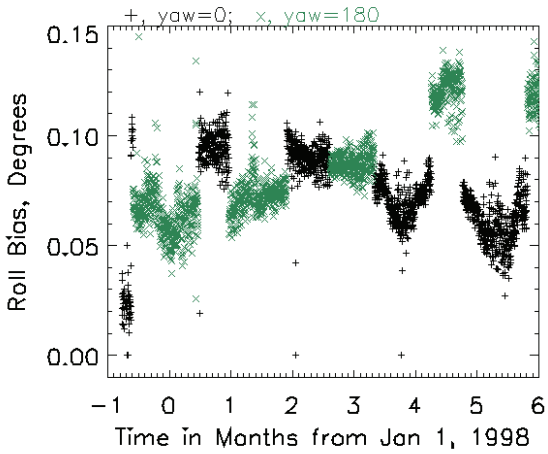

Fig. 9. Early mission roll bias from PR

The PR instrument started collecting data on Dec. 8, 1997, and an uplink of ESA and DSS calibration adjustments was done on Dec. 12 when a bias shift of about 0.08 degrees seemed to occur. There was no requirement to align the ACS relative to the PR, and the PR beam width is 0.7 degrees anyway, but it is noted in retrospect that alignments could have been chosen to center the PR swath if that were desired.

The next day, on Dec. 13, the first yaw turn (from 0 to 180 deg. yaw orientation) was performed, causing another shift in the bias like most subsequent yaw turns. Other DSS calibration refinements uplinked on Feb. 25 1998 were intended to improve yaw update accuracy, and don't show noticable effects on the average roll. As to why the yaw turns show changing affects on the average roll bias, a likely explanation is indicated by the long term trends, as discussed below.

2.5 Long term bias trends

The average PR-measured roll bias from each orbit for the mission to date, including both the pre-boost and post-boost period, are shown in Fig. 10 This illustrates a bias drift and a change in the bias patterns after the control change. Since the bias pattern is different for the two standard flight modes, yaw 0 and 180, those are separated in Fig. 10a and 10b to clarify the differences. We will focus on the pre-boost pattern in this subsection.

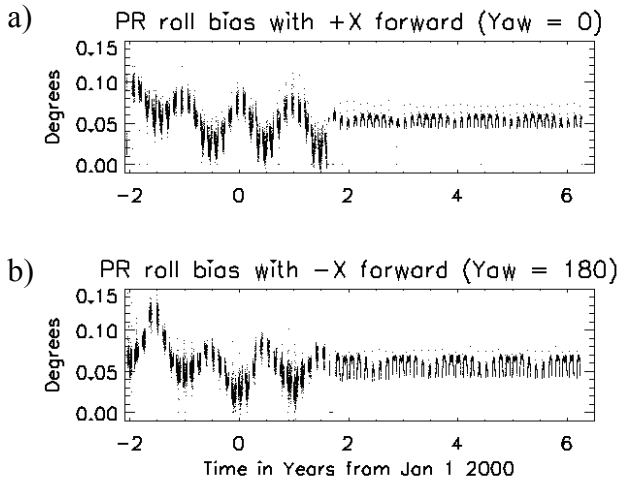

Fig. 10. PR roll bias trends over the mission

Clearly indicated prior to the boost is an annual cycle of about 0.05 degree amplitude with opposite phasing at yaw 0 and 180. Additional evidence that these changes are real is provided by similar offsets inferred from another science instrument—the TRMM Microwave Imager (TMI) [7].

The probable explanation for this is Earth radiance effects, because the maxima occur at the seasonal extremes consistent with a general north-south gradient that changes with season. Other effects may contribute to the error trends however. It is noted that this pattern also shows up in the ground estimated gyro biases, as illustrated later in Fig. 19.

It is possible that the gradual bias drift over the first two years of the mission was due to slight changes in the ESA roll sensitivity, particularly since possible ESA lens fogging was a prelaunch concern. Since this type of degradation would be fixed in the body frame, it wouldn't change sign with yaw turns like the radiance effects. (Note that roll is defined as positive about the +X spacecraft axis whether the yaw is 0 or 180 degrees in the 3-2-1 Euler rotation sequence used.)

3. Post-Boost Control

The TRMM Kalman filter control mode was tested briefly after launch [4], however more details of its performance were learned after the orbit boost [8] when better performance for operational use was desired, and long-term attitude checks were first generated using the PR data for quality assurance.

3.1 Orbit period sinusoidal error pattern

Fig. 11 shows a sample orbit of post-boost roll as computed onboard and computed on the ground using PR data. The only motion shown in the onboard roll (Fig. 11a) are very small disturbances (< 0.02 deg.) from solar array and high gain antennae motions. However the ground computed attitudes (Fig. 11b) show an orbit period sinusoidal error pattern. This pattern was always seen, while the amplitude and phase of the error in the orbit varied only a small amount from orbit to orbit.

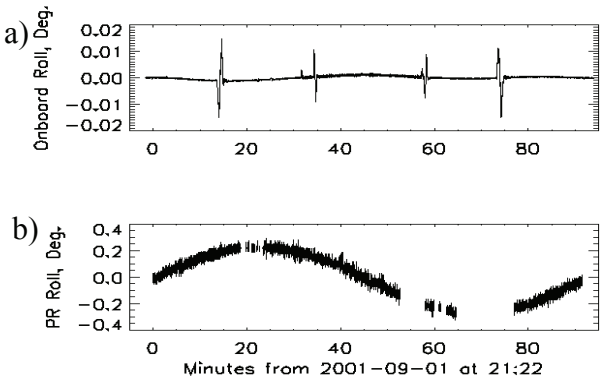

Fig. 11. Onboard, and PR roll for post-boost orbit

This pattern results from the way that onboard errors propagate using gyro data. The attitude propagation is very smooth and reliable with 3-axis gyro data, however initial attitude errors in roll or yaw lead to coupled orbit period roll/yaw errors, with yaw leading roll by one quarter orbit. The error can be thought of as an offset in the estimated direction of the body pitch axis which primarily undergoes 1-rotation per orbit (1-RPO) relative to inertial space. This is not exactly a fixed inertial rotation because the TRMM orbit precesses about -6.7 degrees per day, and TRMM points at the geodetic rather than geocentric nadir. However the control system, using the gyros, tracks those motions, and the residual error in the PR pointing relative to the geodetic nadir always tracks in a sinusoidal pattern.

3.2 Amplitude and phase variations

After the boost, the errors in roll observed by PR were fit with an orbit-period sine wave using each of the orbit-length science data granules. This provided key information for evaluating the performance of the Kalman filter. More recently, these amplitude and phase estimates (including the bias terms plotted in figures 9 and 10) were extended to the whole mission as part of science product reprocessing with algorithm improvements. The amplitude and phases computed from these fits for a year and half around the orbit boost are shown in Fig. 12.

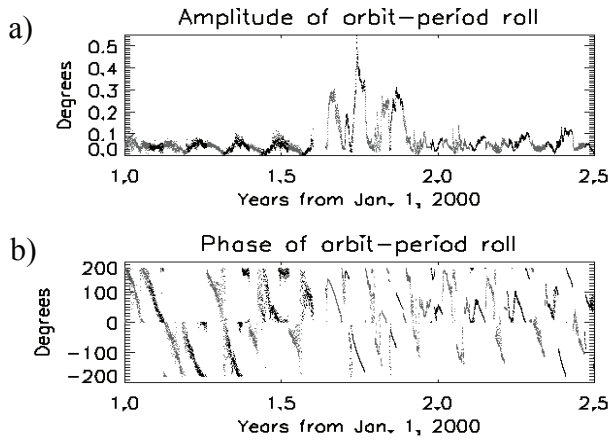

Fig. 12. Amplitude and phase of PR sine signal fits

It is seen that the orbit phase of the maximum error tended to drift at about -7 degrees per day. It was recognized that this relates to the change in the Sun direction in orbit plane. Therefore the phase relative to the Sun direction was computed, and it was seen in data after the boost that the maximum errors tended to be plus or minus 90 degrees in phase relative to the Sun direction. The error magnitudes about and toward the Sun direction are illustrated in Fig. 13 for 200 days following the orbit boost.

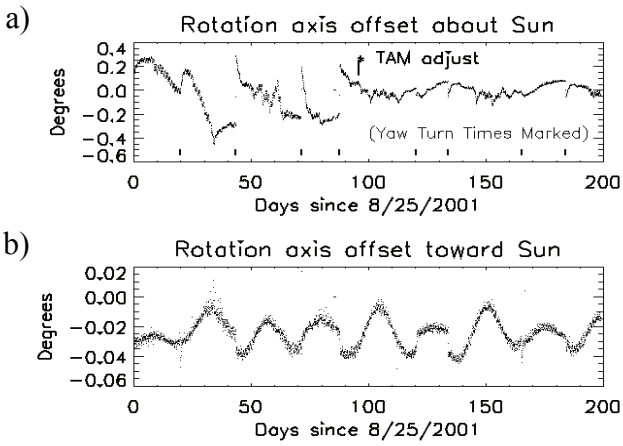

Fig. 13. Post-boost errors relative to Sun direction

This pattern in the pointing offset results from the Sun sensor providing more accurate and stable measurements than the magnetometer. An offset of the pitch 1-RPO rotation axis about the Sun direction keeps the same Sun elevation measurements from the body X-Z plane. That small systematic errors in the Sun elevation measurements from each DSS may vary with β angle probably helps explain the pattern of small errors in the pitch axis toward the Sun direction. At yaw turns the attitude errors typically jump to new values.

3.3 TAM matrix adjustment

Since the pointing was less accurate in a rotation about the sunline, the magnetic field model and TAM calibration were reviewed after the orbit boost. New TAM calibration matrix results did not show significant change from the previous ones, and their uplink did not change the performance noticeably. Further investigation uncovered an error in how the TAM calibration matrix was used onboard. The onboard computations presumed an orthogonal alignment matrix so that the transpose could be taken as the inverse, while the ground computed matrix allowed scale factor and non-orthogonal axis adjustments. A decision was made to uplink the transpose of the inverse of the ground-computed matrix so that proper magnetometer residuals would be computed onboard. This was done on November 28, 2001 (as noted in Figure 13a) and led to improved performance.

3.4 Post-Boost bias trends

As was seen in Fig. 10, the average roll bias variations were much smaller after the boost under Kalman filter control. The roll biases change in a regular pattern with solar β angle, but otherwise show no secular drift. Fig. 14 shows a two month period of the post-boost bias variation.

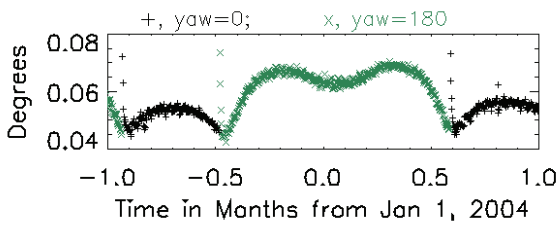

Fig. 14. PR roll bias over 2-month post-boost span

The regular pattern varies roughly with the absolute value of the β angle, but with a reduction in the bias at the largest β magnitudes. This is associated with the elevation of the Sun path from the body X-Z plane. Small systematic errors across the field-of-view of the Sun sensors could drive these effects. In particular, a non-orthogonality of the two axes of DSS-2 led to calibrations optimized for the pre-boost yaw updates [9], and these calibrations may be less optimal for the Kalman filter.

A regular feature of particular note is that the PR-measured roll bias takes a few orbits to settle to a new value after each yaw turn. This is correlated to the settling of the gyro biases calculated onboard by the Kalman filter, as discussed in Section 5.2.

4. Ephemeris Error Effects

After the control change with the orbit boost, onboard ephemeris accuracy became more important for attitude control. Without the direct use of the Earth sensor for pitch and roll pointing, the onboard orbit information was needed to compute the Earth reference direction for control.

4.1 Onboard ephemeris loads and pitch effects

TRMM orbit determination is performed daily on the ground utilizing Tracking and Data Relay Satellite (TDRS) range and Doppler observations. Each day, a state vector from the ground ephemeris is uploaded to the spacecraft. The largest errors in orbit propagation tend to be in the along-track direction. The onboard along-track errors for a sample 15-day period after the orbit boost are shown in Fig. 15. Discontinuities generally show up at each onboard vector load.

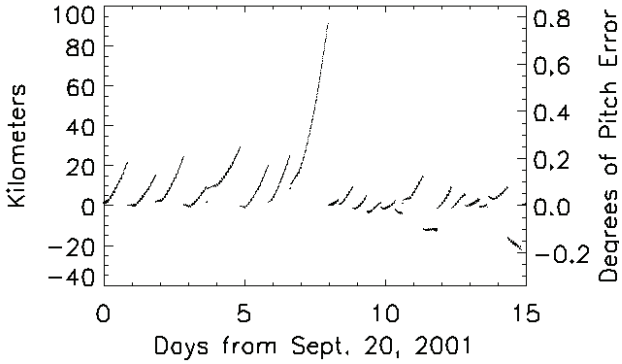

Fig. 15. Onboard along-track error for 15 days

Along-track errors produce a pitch error from the rotation of the orbital reference frame, as indicated by the scale on the right side of Fig. 15. The direct effect on pitch can be seen from the jump in onboard pitch at each vector load, as illustrated in Fig. 16 for the large onboard ephemeris correction near the end of Sept. 27, 2001.

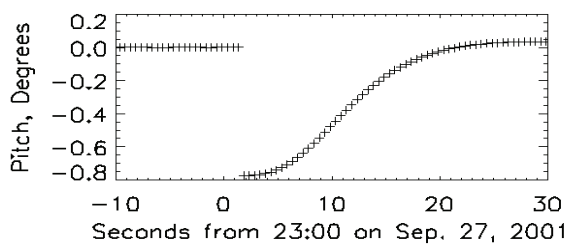

Fig. 16. Onboard pitch error at ephemeris update

The control system responds to null the newly-perceived pointing error within about 20 seconds of the vector upload. The result onboard would seem

to be a pitch error that grows slowly with the along track errors, and then is corrected quickly. However it was noted that the pitch errors can also couple with roll and yaw, as discussed in section 4.3.

4.2 Onboard ephemeris improvements

After the boost, efforts were directed at improving the accuracy of the on-board ephemeris. Increasing the frequency of ephemeris uploads from once per day to twice per day was initiated immediately after the large errors on Sept. 27, 2001, as shown in Fig. 15. This yielded some improvement, but was operationally undesirable.

Attention was focused on the difference between the onboard and ground propagators. The TRMM onboard propagator employs a low-order gravity model and a simplified Jacchia-Roberts 1971 atmospheric density model. It is usually initialized daily using the ground computed state vector and current values of drag correction, exospheric temperature, and geomagnetic index, Kp. Additional improvement was gained by identifying and compensating for an error in application of the ground drag scale parameter in the post-maneuver vector upload. However it became clear more improvement was desirable.

While the ground orbit model incorporates a 30x30 geopotential field, the TRMM onboard propagator only accounts for the J_2, J_3, and J_4 zonal, and $C_{2,2}$ and $S_{2,2}$ sectoral non-spherical terms, a reduced-order propagator employed in a number of Goddard missions. The difference between the ground and onboard geopotential results in an inherent error in propagation of the 30x30 derived state vector on-board TRMM. This error was analyzed in detail for this onboard model in a study by Mark Beckman [9] that showed the error may be minimized by selecting upload epochs to be at a time when the spacecraft crosses an equipotential of the ground and onboard field models. This improvement was implemented on January 7, 2002 and is associated with the largest marked improvement in routine onboard ephemeris accuracy. These improvements can be seen by comparing Fig. 15 with Fig. 18b, disregarding the loads following orbit adjusts. The orbit adjust times can be seen in the plots from the very short segments between discontinuities, for the 45 minute periods between burn pairs.

Finally, it was observed that some of the worst onboard ephemeris errors were associated with uploads from ground ephemeris generated on the day of an orbit-adjust maneuver. The quality of the ground ephemeris on the day of a maneuver was improved by incorporating the actual finite maneuver plan in the ephemeris on maneuver days. Prior to this change, only a coarse maneuver plan was included in any ephemeris delivered for a daily upload. The coarse plan could be incorrect by a few minutes in burn start/stop times and a few seconds in duration when compared to the actual finite burn plan executed on TRMM. Since the finite burn plan for a TRMM maneuver is generated and delivered on the day before a maneuver, it was possible to use the finite burn plan in ephemeris generation on the maneuver day, rather than the coarse plan. This change was put into place on January 30, 2002.

The effects of these changes may be seen in Fig. 17. Improvements have kept the onboard ephemeris errors generally below 10 kilometers. Rare cases of larger error have been associated with geomagnetic storms which affect atmospheric drag levels. One period of slightly higher errors near the end of 2002 occurred when a solar array drive anomaly forced the feathering (edge-on to the velocity placement) of one solar array. The effects of changes in cross sectional area were incorporated after it was decided to keep that array feathered.

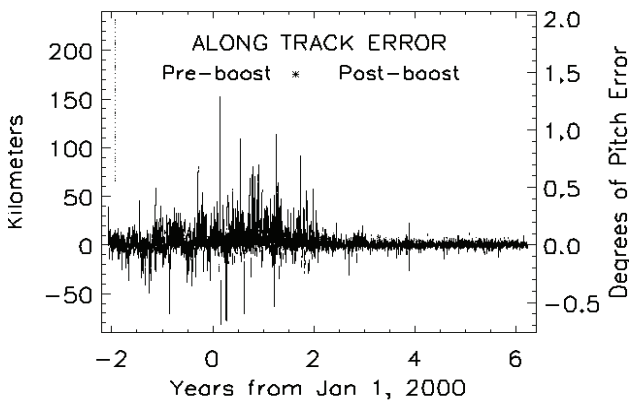

Fig. 17. Onboard ephemeris error since launch

4.3 Ephemeris error effects on roll/yaw

Ephemeris errors were observed to have secondary effects on roll and yaw, especially during high β angle when pitch effects can couple into roll and yaw. Examples of this effect are shown in Fig. 18, where the rotation axis shift about the sunline (as discussed with Fig. 13) is shown along with onboard ephemeris errors for that time span. The solar β angle reached about 55 degrees below the orbit plane around Jan. 20, 2002 (while being near zero

on Jan. 6 and Feb. 6). A rotation about the sunline changes the spacecraft pitch by an amount that varies as the sine of the β angle. Thus, around the high β angles, pitch errors can couple into roll/yaw offsets which are related to rotation axis offsets

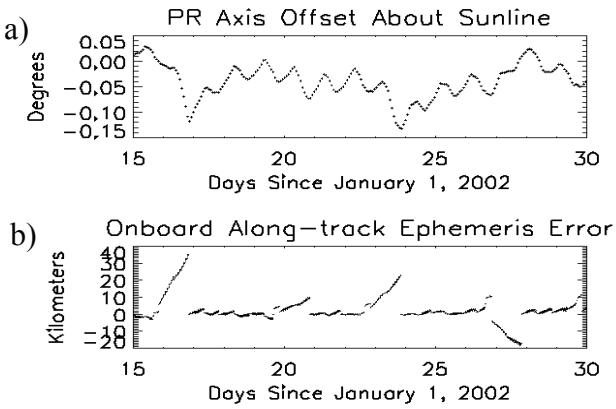

Fig. 18. Axis offset associated with ephemeris error

Another effect on the Kalman filter of along track errors would be that the predicted magnetic field vectors used in computation of TAM measurement residuals would have errors. However this was not a dominant effect because little effect of ephemeris error on roll/yaw was seen when β was near zero.

5. Gyro Bias Estimates

Gyro biases estimated by various methods show noteworthy correlation with the orbital average roll biases observed using the Precipitation Radar.

5.1 Ground computed gyro biases

TRMM attitude determination is performed on the ground once per week for the purpose of monitoring the performance of the onboard attitude. The TRMM ground attitude solution now utilizes a two-orbit arc of sensor data in its batch least-squares estimation, though prior to the orbit boost a one-orbit arc was usually used. The two-orbit arc was found to be more consistent during post-boost attitude error analysis. Gyro biases are estimated simultaneously with the TRMM attitude at the epoch time. Results for these gyro biases since launch are shown in Fig. 19. Early mission results for these biases were reported previously [6], but now very long term trends are seen. The causes of all of these trends are not currently understood, but some observations about them are noted. Separated values occur at 0 and 180 degree yaw orientations. The shifts at yaw turns can result from small residual sensor alignment or calibration errors.

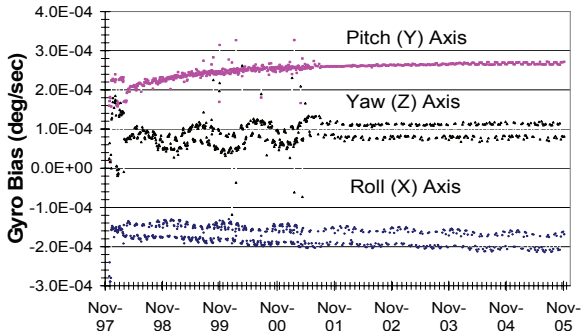

Fig. 19. Ground computed gyro biases

Of particular note is that the yaw component of the gyro drift bias shows an annual cycle that disappears after the control change at the orbit boost. This is similar to the effect seen in the PR roll bias (see Fig. 10). This indicates correlation of roll bias effects with yaw gyro drift bias effects in the attitude solutions. The correlation changes sign at yaw turns as the rate biases combine with opposite pitch rates. Additional effects of various sensor errors may contribute to these trends, as well as bias drift from the gyros themselves. Temperatures of the gyros were examined and do not show correlation with these trends. Possibly some effects might result from mass property changes as spacecraft fuel was used. Further analysis of these long term trends could be informative in separating possible causes.

5.2 Onboard gyro bias correlation with roll bias

The Kalman-filter-computed yaw gyro biases take several orbits to settle to new values after each yaw turn. A representative plot of the onboard yaw gyro drift bias around a yaw turn is shown in Fig. 20.

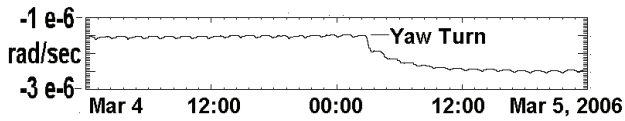

Fig. 20. Onboard yaw rate bias change at yaw turn

Following a quick shift after the yaw turn, the yaw gyro bias value takes several orbits to drift to a nearly steady-state value. The PR roll bias similarly takes several orbits to settle (see Fig. 14). The magnitude of the PR bias after the yaw turn is consistent with the offset expected from the gyro bias by a vector addition with the basic 1-RPO rate. While the drift bias is settling, the ACS seems to rotate the body frame about an axis that is offset by roughly the amount of the residual roll error, with this axis near the orbit axis. This correlation merits further review for both short and long-term trends.

6. Conclusions

The Kalman filter control mode using Sun sensors, magnetometers and gyros has performed as well or better than the original control, allowing TRMM to successfully continue its extended mission after the orbit boost. This was achieved after improving the onboard ephemeris loads and adjusting an onboard magnetometer calibration matrix. Various aspects of the pointing performance have been verified by using the PR science instrument. Occasional Sun interference effects gave the largest errors in the pre-boost period. The mode switch exchanged occasional short-term interference and systematic radiance effects from the horizon scanner for much smoother control with orbit period errors. Under Kalman filter control, offsets of the rotation axis tend to occur about the Sun direction giving coupled roll/yaw orbit period errors. Ephemeris errors can cause pitch errors, which will also exacerbate roll/yaw errors at high sun elevation angles. An association between roll biases and yaw gyro drift rate biases is demonstrated in flight data. Very long term error trends have been noted, some of which changed with the control changes.

7. Possible Future Work

Further understanding of the residual patterns, trends, and correlations could help clarify error indicators and performance expectations for future missions or alternate ground processing algorithms. TRMM science products currently use the onboard attitude which has known errors as described here. Many TRMM science algorithms do not need better than 1-pixel-accuracy geolocation, but some newer algorithms are notably sensitive to Earth-viewing incidence angle, and could benefit from a ground definitive attitude.

8. Acknowledgements

The authors wish to acknowledge the help of staff at the NASA Goddard Space Flight Center TRMM Science and Data Information System, Flight Dynamics Facility, and Flight Operations Team that supported this work. In particular thanks are extended to John Stout and Charles Cosner for staging science data for trending efforts, to Owen Kelley for assistance with data plots, to Joseph Kowalski for ACS trending data, and to Joseph Hashmall, Joseph Sedlak, Gregory Natanson, Stephen Andrews, and Frederick Patt for helpful discussions.

References

[1] Adler, R., et. al., "TRMM Senior Review Proposal 2005," available at http://trmm.gsfc.nasa.gov/

[2] Kelley, O.A., and J. Stout, "Convective towers in eyewalls of tropical cyclones observed by the TRMM Precipitation Radar in 1998-2001," Extended Abstracts, 20th Conference on Weather Analysis and Forecasting, Seattle, WA, USA, 2004.

[3] Crassidis, J.L., S.F.Andrews, F.L. Markley, and Kong Ha, "Contingency Designs for Attitude Determination of TRMM," NASA/GSFC Flight Mechanics Symposium NASA/CP 3299, Greenbelt, MD, May 1995.

[4] Andrews, S.F. and W.M. Morgenstern, "Design, Implementation, Testing, and Flight Results of the TRMM Kalman Filter," AIAA 98-4509, Aug. 1998.

[5] Kwiatkowski, J., S. Bilanow, and J. Stout, "Estimating TRMM Spacecraft Attitude Errors Using the Precipitation Radar." IEEE International Geoscience and Remote Sensing Symposium, Toronto, Canada. June 2002.

[6] Robertson, B., S. Placanica, W. Morgenstern, J. Hashmall, J. Glickman, G. Natanson, "On-orbit Performance of the TRMM Mission Mode," 14th International Symposium on Space Flight Dynamics, Foz do Iguaçu, Brazil, February 1999.

[7] Bilanow, S., and F. S. Patt, "Correlated Errors in Earth Pointing Missions." NASA/GSFC Flight Mechanics Symposium, Greenbelt, MD, USA, October 2005.

[8] Andrews, S.F. and S. Bilanow, "Recent Flight Results of the TRMM Kalman Filter," AIAA Guidance Navigation and Control Conference, AIAA 2002-5047, Monterey, CA, USA, August 2002.

[9] Natanson, G., "Calibration of the Misaligned Heads of the Digital Two-Axis Sun Sensor for the Tropical Rainfall Measuring Mission," Computer Sciences Corporaton, CSC-96-968-05, February 2000.

[10] Beckman, M., "Reducing On-Board Computer Propagation Errors Due to Omitted Geopotential Terms By Judicious Selection of Uploaded State Vector," Flight Mechanics/Estimation Theory Symposium, Greenbelt, MD, USA, 1996.